ISSN 0040-5795, Theoretical Foundations of Chemical Engineering, 2021, Vol. 55, No. 1, pp. 41–52. © Pleiades Publishing, Ltd., 2021.
Russian Text © The Author(s), 2021, published in Teoreticheskie Osnovy Khimicheskoi Tekhnologii, 2021, Vol. 55, No. 1, pp. 46–57.

Analysis and Simulation of the Motion of Particles near the Heat Exchange Surface Immersed in a Fluidized Bed

O. Yu. Milovanov[a], *, R. L. Is'emin[a], D. V. Klimov[a], V. S. Kokh-Tatarenko[a], and O. M. Larina[b]

[a] *Tambov State Technical University, Tambov, Russia*

[b] *Joint Institute of High Temperatures, Russian Academy of Sciences, Moscow, Russia*

**e-mail: penergy@list.ru*

Received March 30, 2020; revised June 15, 2020; accepted June 18, 2020

Abstract—The immersion of a heat exchanger into a fluidized bed changes the hydrodynamic structure of the bed, which, according to this study, has a decisive influence on the heat transfer process. A near-surface zone with a local vertical circulation of particles and a porosity that is higher than that in the rest of the bed volume is formed near the immersed body with an increase in the velocity of the gas blown through the bed. As is shown in this study, the deterioration of the exchange of particles between this zone and the rest of the bed volume leads to a decrease in the intensity of external heat transfer with an increase in the gas velocity. A model is proposed that makes it possible to calculate the width of the near-surface zone and the time of residence of fluidized bed particles in it.

Keywords: fluidized bed, heat transfer surface, particle motion, near-surface zone, residence time of particles in the near-surface zone

DOI: 10.1134/S0040579520060172

INTRODUCTION

The residence time of a particle near the heat transfer surface immersed in a fluidized bed must be determined to calculate the intensity of external heat transfer in a fluidized bed by means of all the proposed heat transfer models [1–9].

Table 1 lists the methods of determination and the values of the residence time of particles near the heat exchange surface which were obtained in previous studies.

The scatter of the values of the residence time of particles near a heat exchange surface when they are determined by different methods draws attention (Table 1). On the other hand, the correctness of determining this parameter is of great importance.

In particular, the parcel heat transfer model still widely used [4, 5] gives an unrealistic relationship between the heat transfer coefficient and the heat capacity of solid particles [11, 19], and the heat transfer coefficient predicted by the parcel model increases to infinity with a decrease in the time of residence of particles near the heat exchange surface [6, 11]. To overcome the drawbacks of the parcel model, an additional thermal resistance is introduced between the fluidized bed and the heat exchange surface (gas film) [20–23], which generates additional uncertainties in the parcel model. On the one hand, the gas film thicknesses determined in different models are very different for apparently similar conditions [24]. On the other hand, it was proved that the existence of such a gas film contradicts the physical reality [1, 25].

The alternative particle-based model is free from the drawbacks of the parcel model, since it is not associated with modeling the properties of mythical parcels and the introduction of a nonexistent thermal resistance in the form of a gas film [10, 24].

However, the lack of detailed information on the motion of individual particles near the wall in the open literature sources hinders the further development of this model.

On the other hand, it has been proven experimentally that the placement of heat exchanger tubes in a fluidized bed changes the hydrodynamic structure of the bed. A precessing gas cavity is formed under a vertically immersed body, which periodically generates gas bubbles that rise both along the immersed body and at a certain angle to it. As a result, a certain zone of the bed with local circulation of particles in it is formed near the immersed body, i.e., a heat transfer surface, which has a width equal to several diameters of particles and an increased porosity [26, 27]. This region of the bed will be further referred to as the "near-surface zone"; owing to the higher porosity, part of the gas rushes into this zone, which gives rise to a decrease in the gas velocity in the rest of the bed [28]. Obviously, the rate of exchange of particles between the near-surface zone and the rest of the bed should

Table 1. Applied methods and results of determining the residence time of particles at the heat exchange surface

Method used for determination	Time of residence particles at the heat exchange surface	Literature source
Observation of temperature fluctuations in platinum foil	0.15–1.0 s	[5]
	0.1–0.5 s	[14]
Extrapolation from the time of residence of particles in stirred beds	1–1.6 s	[10]
Video recording of labeled particles	≈3 s	[11]
	0.02–0.36 s	[12]
Analysis of the video of particle motion	1.5–6.0 s	[13]
	0.04–0.08 s	[16]
	0.5–5 s	[1]
Analysis of fast-response capacitive sensor signals	0.07–1.13 s	[15]
Detection of particle radiation with an infrared camera	0.35–0.5 s	[18]

affect the rate of heat transfer between the immersed surface and the fluidized bed.

The aim of this work was to study the process of formation of a near-surface zone and the exchange of particles between this zone and the rest of the bed, as well as to develop a model for calculating the residence time of particles in the near-surface zone.

EXPERIMENTAL

Experimental Procedures

We studied the motion of aluminosilicate catalyst particles (particle diameter 2.5–3.0 mm and critical fluidization velocity $v_{mf} = 0.86$ m/s) in an apparatus with an inner diameter of $D = 172$ mm. The bed of aluminosilicate catalyst particles was fluidized with air at room temperature.

To elucidate the effect of an immersed body on the movement of particles in a fluidized bed, a comparative study of the movements of particles in a free fluidized bed and in a fluidized bed containing an immersed body that simulated a heat transfer surface was carried out.

In the latter case, a stainless steel cylinder with a diameter of $d = 40$ mm was immersed in the apparatus along the longitudinal axis. The cylinder had a rounded bottom end; the distance from this end to the air distribution grid was 10 mm.

The motion of the particles within the bed was analyzed tracking the magnetically labeled particle introduced into the bed, which was obtained by sintering a ferromagnetic powder and polypropylene. This magnetically labeled particle had the same size and mass as the rest of the particles in the bed. The magnetic moment of the particle after magnetizing in a constant magnetic field was 0.39 A/m. Magnetometers continuously measuring the change in the strength of the magnetic field were installed outside the apparatus, which made it possible to further calculate the coordinates of the particle. The magnetometers were equipped with magnetosensitive sensor units assembled of double-rod differential fluxgates. Each measuring channel had the following characteristics: measurement range $\pm 500 \times 10^{-4}$ Oe, sensitivity 0.02 V/500×10^{-4} Oe, nonlinearity 5%, and supply voltage 10 V. The output signals of the magnetometers were recorded on a computer, and then the components of the particle movement vector in the fluidized bed were determined.

The experiments were carried out at fixed bed height values equal to $H_0 = 0.25D$, $H_0 = 0.5D$, and $H_0 = 1.0D$ and the air velocity values equal to $1.5v_{mf}$, $2.5v_{mf}$, and $3.5v_{mf}$. The error in determining the coordinates of the labeled particle was ±10%.

The movements of the particle along the vertical $Z(t)$ and along the radius $R(t)$, which were counted from the apparatus center, were studied. Then, the trajectories of the particle movements along the vertical and radius were divided into separate segments every 0.2 s. This made it possible to determine the values of particle velocity vectors v_Z and v_R by the method of numerical differentiation.

To determine the probability of finding a particle in different points in the bed, the entire volume of the bed was divided into cells with a size of 10 × 10 mm, and the number of occurrences of the particle in each cell was calculated. On the basis of these data, probability distribution histograms for the probability of finding particles in any point in the bed were constructed.

In order for the results of an analysis of tracking the motion of one particle to be extended to the movements of all particles in the bed, the duration of observation of an individual particle has to be twice the effective correlation time numerically equal to the area under the curve of the normalized correlation function of the $R(t)$ (or $Z(t)$) random process. In the course of preliminary experiments, it was found that this area is

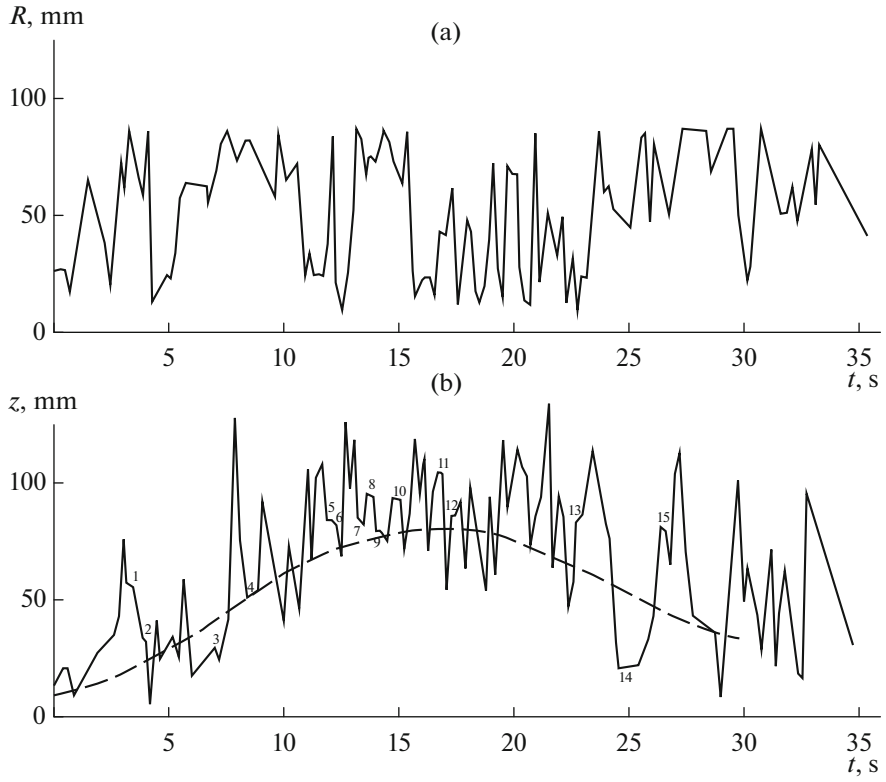

Fig. 1. Sections of the particle-trajectory projections onto the (a) horizontal and (b) vertical planes in a free bed ($H_0 = 0.5D$ and $v = 1.5v_{mf}$).

maximum for the $R(t)$ random process at $H_0 = 1.0D$ and $V = 1.5v_{mf}$.

It was found that the time of observation of a magnetically marked particle in each experiment should be at least 78 s; the actual observation time was 100 s. With such an observation time, the point at which the labeled particle was introduced into the bed and the way it was introduced into the bed do not matter.

Analysis of the Obtained Data

The results of analyzing the motion of particles as they were in a free fluidized bed showed that this process in a free bed depends on the rearrangement of the air velocity profile over the cross sections of the bed with distance from the air distribution grid.

In actual fact, the air velocity profile, which is initially flat at a low height of the free fluidized bed on the air distribution grid, transforms, with distance from the latter, into a convex velocity profile with a maximum near the center of the apparatus, as is shown in [29]. Moreover, the higher the air velocity with respect to the empty section of the apparatus, the faster this transformation occurs. This led the authors of [29] to assume that a fluidization site with local vertical circulation of solid phase particles is spontaneously formed in the fluidized bed.

The study of the motion of particles in a free fluidized bed confirmed this assumption.

Segments of the trajectory of a labeled particle in a free fluidized bed are shown in Figs. 1–3, which are projected onto the horizontal (parts (a) of the figures) and vertical (parts (b) of the figures) planes at air velocities v of 1.5, 2.5, and $3.5v_{mf}$ and an initial bed height of $H_0 = 0.5D$.

This motion is superimposed on sharp fluctuations in the trajectory of the particle moving near the upper boundary of the bed, which are obviously caused by the release of air bubbles to the bed surface and their extinction. With an increase in the air velocity to $v = 2.5v_{mf}$, the period of the vertical circulation of particles decreases to 15 s; at an air velocity of $v = 3.5v_{mf}$, this period decreases to 4.2 s.

With an air velocity of $v = 1.5v_{mf}$, the particle is approximately equally likely to be found at any point of the radius of the apparatus.

With an air velocity of $v = 2.5v_{mf}$, the probability of finding particles in a ring between radii of $R = 30$ and 60 mm increases.

With an air velocity of $v = 3.5v_{mf}$, this ring narrows and is limited by radii of $R = 20$ and 40 mm.

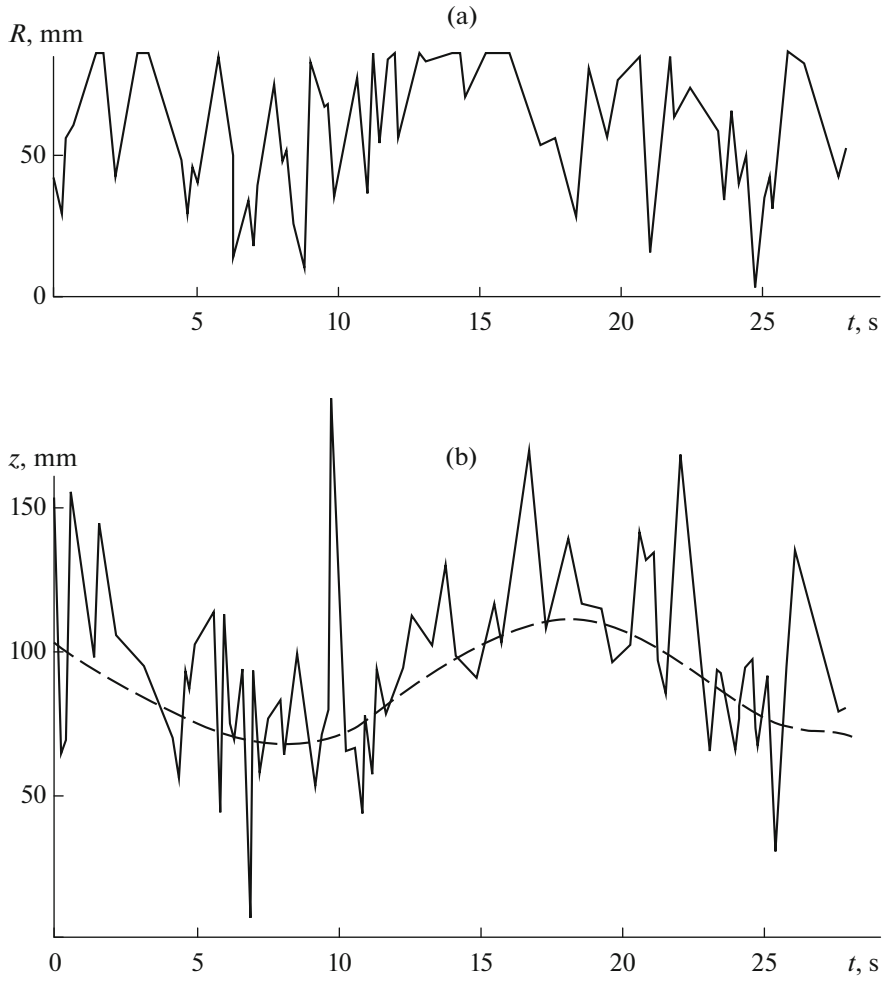

Fig. 2. Sections of the particle-trajectory projections onto the (a) horizontal and (b) vertical planes in a free bed ($H_0 = 0.5D$ and $v = 2.5v_{mf}$).

At the same time, the probability of imparting a radial velocity component close to zero to particles increases with an increase in the air velocity.

This kind of particle motion confirms the appearance of a focal fluidization regime with local vertical circulation of particles in a narrow ring with an increase in the air velocity in a free fluidized bed.

A decrease in the initial bed height to $H_0 = 0.25D$ gives rise to the appearance of a fluidized zone near the ring with an average radius of 45 mm just at an air velocity of $v = 1.5v_{mf}$.

An increase in the initial bed height to $H_0 = 1.0D$ leads to the degeneration of the focal fluidization regime with an increase in the air velocity, so the probabilities of finding particles at different points of the apparatus radius become approximately equal.

The placement of a vertical cylinder in the bed redistributes the air flows in the latter and leads to the occurrence of focal fluidization near the body immersed in the bed.

Figure 4 shows the segments of the particle trajectories in a bed with a vertical cylinder along the radius and along the vertical at an air velocity of $v = 1.5v_{mf}$ and an initial bed height of $H_0 = 0.5D$.

As follows from Fig. 4, the particle moves freely over the entire cross section of the bed with the above air velocity, but it is more likely for the particle to be found near and above the boundary of the fixed bed.

At the same initial bed height, an increase in the gas velocity to $3.5v_{mf}$ increases the probability of finding particles in the near-surface zone limited by radii of 20 and 40 mm; the probability of finding particles in the part of the bed cross section with a radius of $R >$ 50 mm decreases (Fig. 4). Segments of the trajectory of the particle movement temporarily localized in the near-surface zone, in which the particle makes lifting and lowering motions and then leaves the near-surface zone, can be seen in Fig. 4.

Interestingly, it is more likely that the radial component of the particle velocity at a gas velocity $3.5v_{mf}$

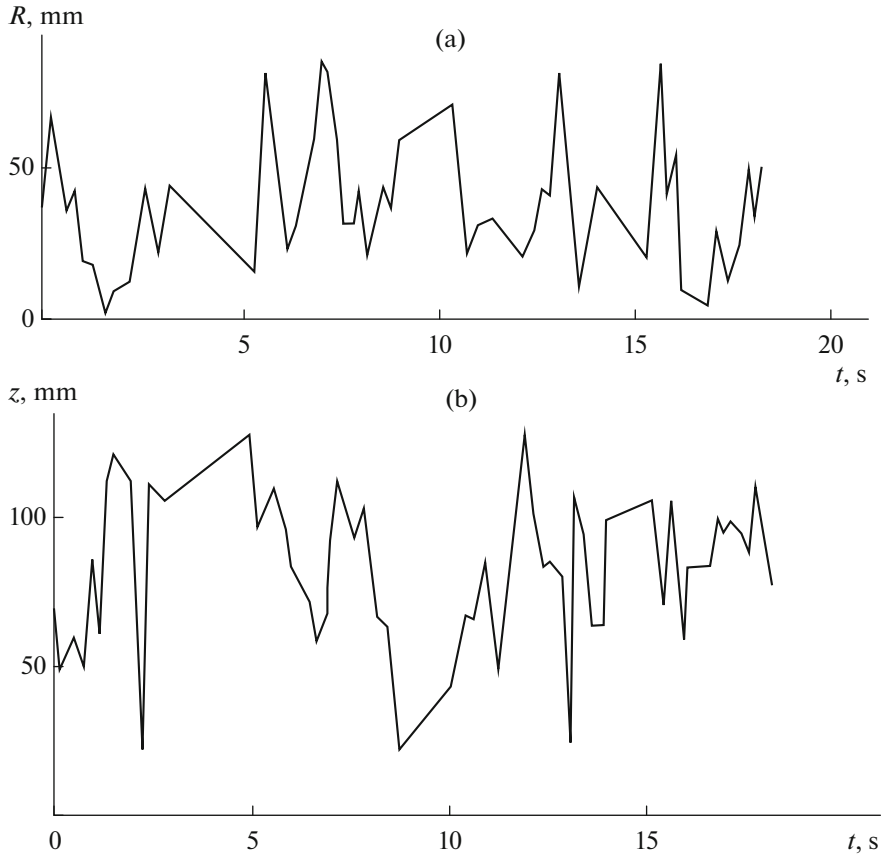

Fig. 3. Sections of the particle-trajectory projections onto the (a) horizontal and (b) vertical planes in a free bed ($H_0 = 0.5D$ and $v = 3.5v_{mf}$).

equals $v_R \approx 0$ mm/s (Fig. 5). At the same time, the particles often have a radial velocity of $v_R = \pm 40$–80 mm/s at lower values of the gas velocity (Fig. 5), while the probabilities of imparting negative and positive velocities to particles are approximately equal.

The described observations suggest that the formation of a near-surface zone at the initial bed height occurs at an air velocity of $3.5v_{mf}$. In this case, focal fluidization of particles located in the near-surface zone there is observed, as is evidenced by a radial velocity value equal to $v_R \approx 0$.

A decrease in the initial bed height to $H_0 = 0.25D$ leads to a sharp increase in the probability of finding particles near the cylinder in a region with a width of 10–20 mm just at $v \le 2.5v_{mf}$; in this region, a near-surface zone is formed.

Upon an increase in the initial height to $H_0 = 1.0D$, no pronounced near-surface zone is observed in the investigated range of air velocities—the probability of finding particles in the region of $R > 50$ mm at $H_0 = 1.0D$ and $v = 3.5v_{mf}$ is higher than that at the same gas velocity but a bed height of $H_0 = 0.5D$.

Before the formation of the near-surface zone, the time spent by the particles near the immersed body is 0.35–0.4 s at a distance of up to 20 mm from the body and 0.3–0.38 s at a greater distance from the immersed body.

After the formation of the near-surface zone, the residence time of particles in it is 0.36–0.5 s (these values are close to the experimental data obtained in [12, 14, 18]), and the residence time outside the near-surface zone is 0.25–0.4 s.

Thus, the formation of the near-surface zone with the width equal to 7–8 of the average particle diameter of the bed has no substantial effect on the residence times of particles in this zone and outside it. However, the formation of the near-surface zone has a substantial effect on the circulation of particles in the radial direction—before the formation of the near-surface zone, there is intense circulation of particles in the radial direction, which is not observed after the formation of the near-surface zone.

This should have an effect on the intensity of heat transfer between the fluidized bed and the body immersed in it.

This assumption is confirmed by experimental data. Figure 7 shows the curves of changes in the intensity of heat transfer between a fluidized bed of aluminosilicate catalyst particles with a diameter of

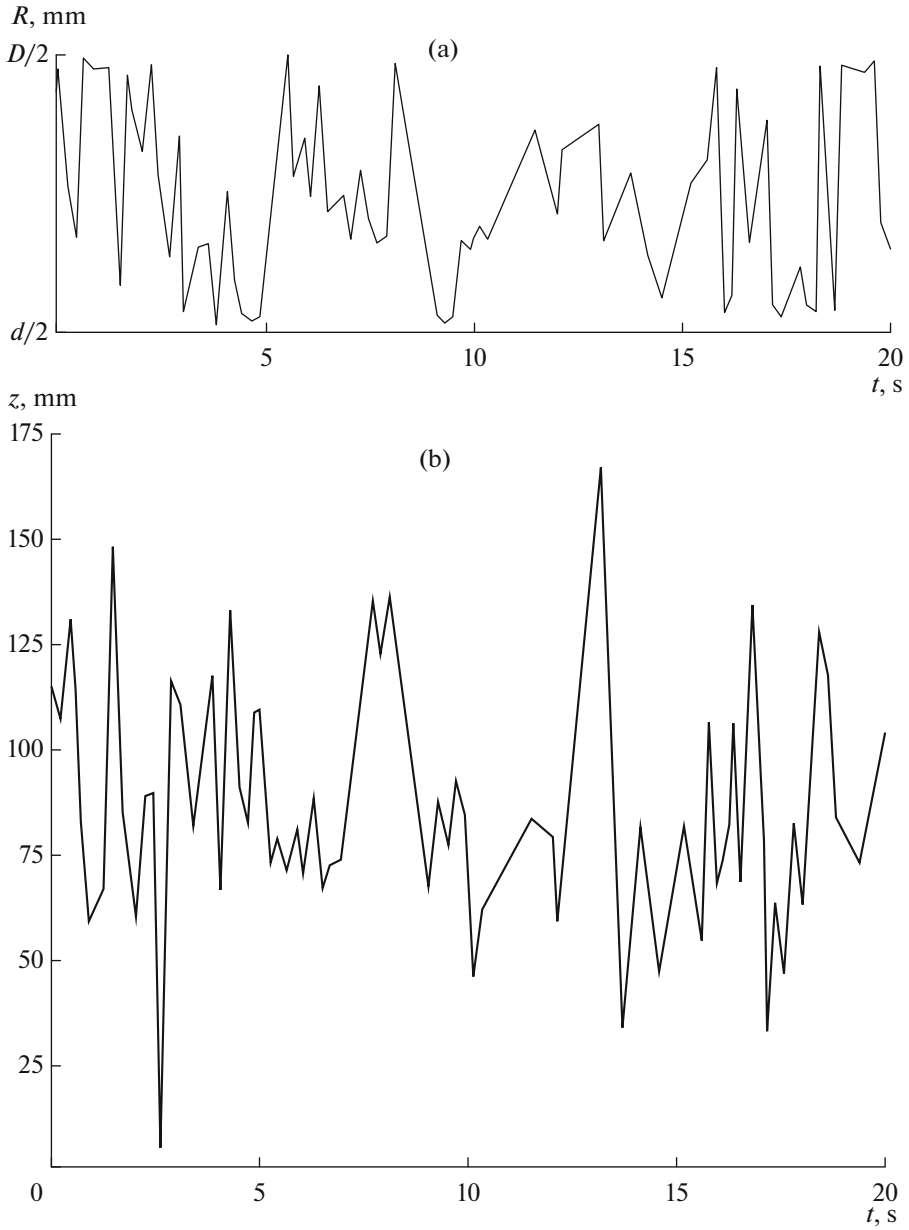

Fig. 4. Particle-trajectory projections onto the (a) horizontal and (b) vertical planes in a bed with a vertical cylinder at a velocity of $v = 1.5v_{mf}$ and an initial bed height of $H_0 = 0.5D$.

2.5–3.0 mm and a vertical heater with a diameter of 40 mm at air velocities of 1.5, 2.5, 3.5, and $4.5v_{mf}$ [30].

As is seen from Fig. 7, the intensity of heat exchange between the fluidized bed and the heater increases until the air velocity reaches $3.5v_{mf}$, i.e., until the formation of a near-surface zone, after which the intensity of heat transfer decreases. Thus, the reason for the extreme dependence of the intensity of heat transfer between the fluidized bed and the surface immersed in it is the formation of a near-surface zone and the cessation of intensive circulation of particles in the radial direction.

Calculation of the Residence Time of Particles in the Near-Surface Zone

As was found in the course of the experiments described above, there is a local blow-out of particles in the near-surface zone. Under certain conditions, these circulation flows can be described using the mechanics of circulation flows in an ideal incompressible fluid.

Let us assume that the porosity of the bed in the near-surface zone is constant and equals ε. In this case, the vector equations of hydromechanics of a steady-state fluidized bed are expressed as follows [31]:

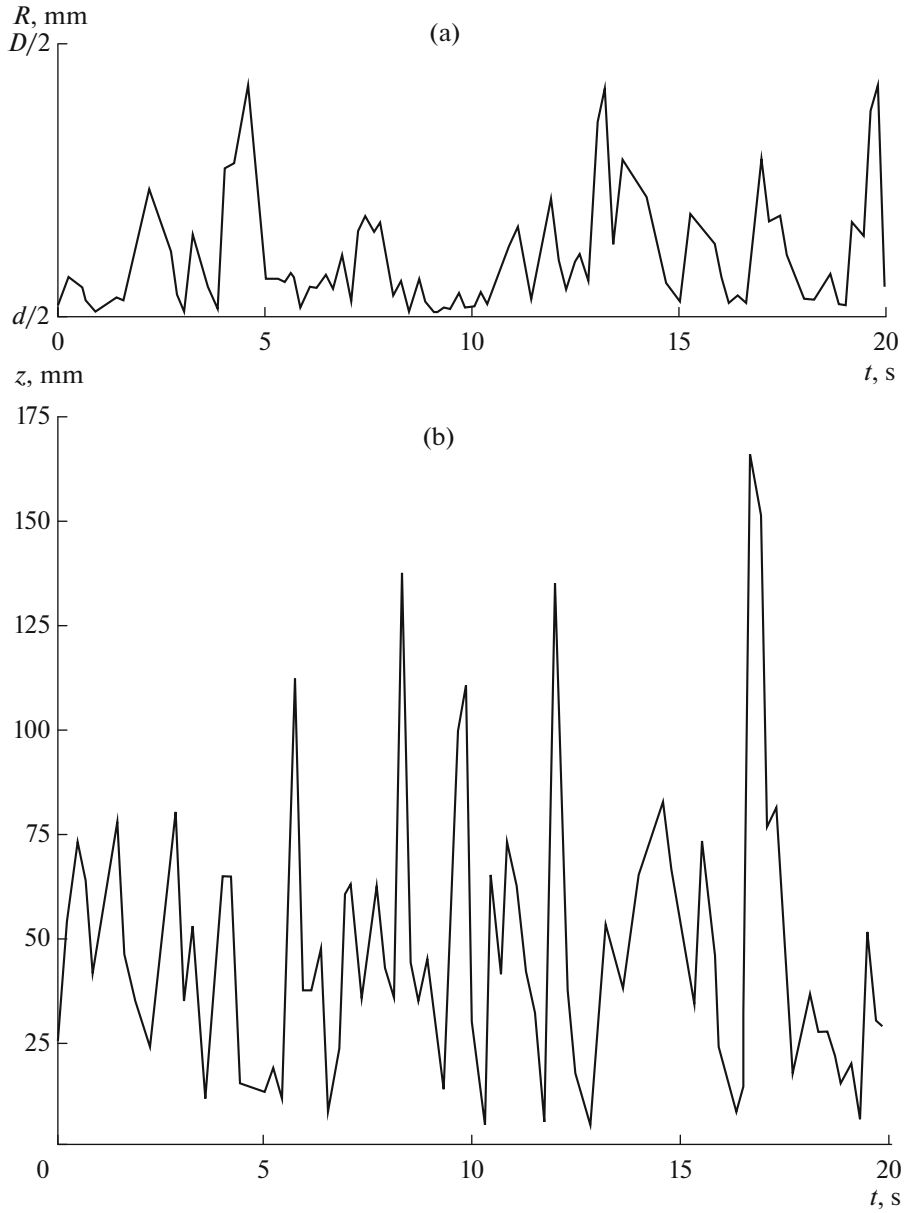

Fig. 5. Particle-trajectory projections onto the (a) horizontal and (b) vertical planes in a bed with a vertical cylinder at a velocity of $v = 3.5v_{\mathrm{mf}}$ and an initial bed height of $H_0 = 0.5D$.

$$\nabla \mathbf{v}_f = 0, \tag{1}$$

$$\nabla \mathrm{v}_s = 0, \tag{2}$$

$$\beta(\varepsilon)(\mathbf{v}_f - \mathbf{v}_s) = 0, \tag{3}$$

$$\rho_s(1-\varepsilon)\left[\frac{d\mathbf{v}_s}{d\tau} + \mathbf{v}_s\nabla\mathbf{v}_s\right] = \nabla(p + p_s) + \rho_s(1-\varepsilon)g\mathbf{i}. \tag{4}$$

Equation (4) has the form of a dependence that describes the motion of an ideal incompressible fluid with a density of $\rho_s(1-\varepsilon)$ and a pressure of $p + p_s$. Let us consider the motion of particles in the x–y plane.

We introduce solid phase stream function ψ_s in the following way:

$$v_{sx} = \frac{d\psi_s}{dx}, \quad v_{sy} = \frac{d\psi_s}{dy}. \tag{5}$$

The equation of this function for the planar problem has the following form [30]:

$$\frac{d^2\psi_s}{dx^2} + \frac{d^2\psi_s}{dy^2} + F'(\psi_s) = 0, \tag{6}$$

where

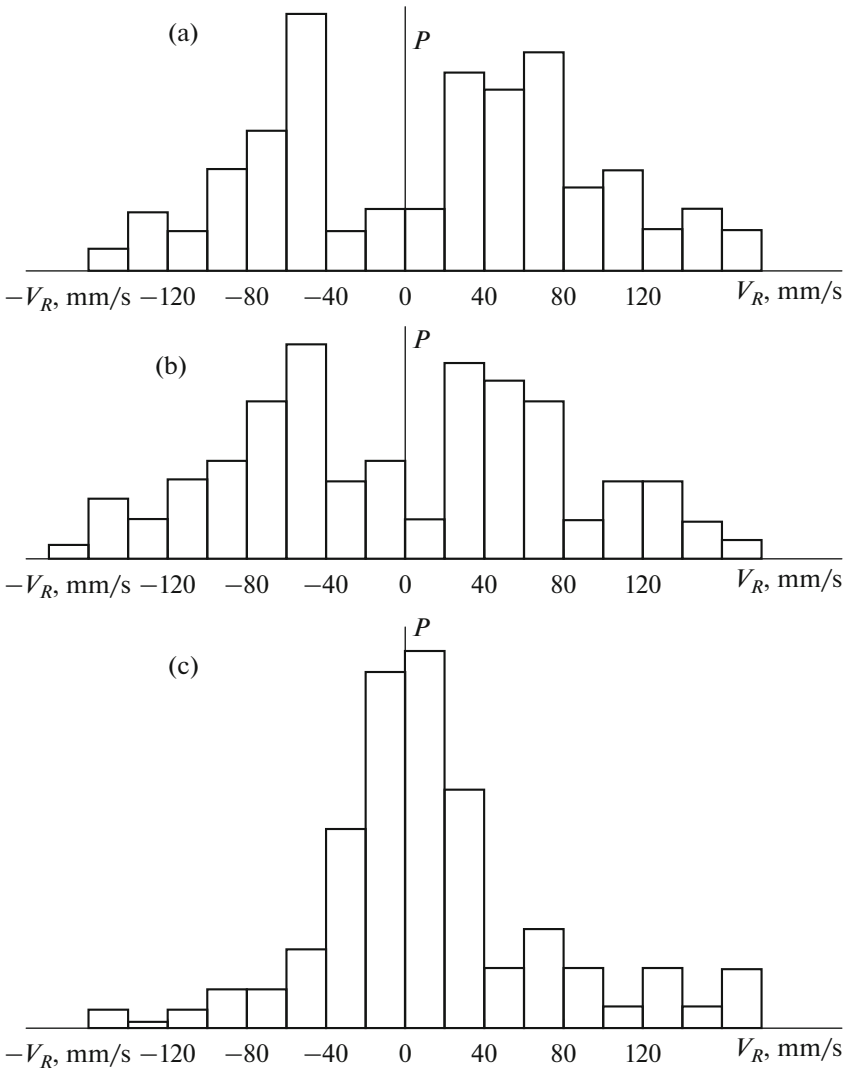

Fig. 6. Estimation of the probability distribution density of the V_R values in a bed with a vertical cylinder at $H_0 = 1.0D$ for (a) $v = 1.5v_{mf}$, (b) $v = 2.5v_{mf}$, and (c) $v = 3.5v_{mf}$.

$$F(\psi_s) = -\frac{v_{sx}^2 + v_{sy}^2}{2} - \frac{p + p_s}{\rho_s(1-\varepsilon)} - gx. \qquad (7)$$

To solve Eq. (6), it is necessary to choose the boundary conditions.

Figure 8 shows the real (geometric) and hypothetical (based on the kinematics of particles) location of the body immersed in the fluidized bed.

The latter is represented taking into account the distribution of particles over the bed height, i.e., assuming the low probability for particles to be found in the lattice zone, which allows us to draw the following conclusion:

$$\psi_s = 0 \quad \text{at} \quad x = 0(h_r). \qquad (8)$$

The validity of expression (8) at $x = H$ is obvious.

Let

$$\psi_s = 0 \quad \text{at} \quad y = 0 \quad \text{and} \quad y = r_{zone}. \qquad (9)$$

Taking into account conditions (8) and (9), Eq. (6) has the following solution:

$$\psi_s = A_n B_m \sin\left(\frac{n\pi x}{H}\right)\sin\left(\frac{m\pi Y}{r_{zone}}\right). \qquad (10)$$

Given that our studies have shown that there is only one circulation loop in the near-surface zone, we obtain

$$\psi_s = A_1 B_1 \sin\left(\frac{\pi x}{H}\right)\sin\left(\frac{\pi y}{r_{zone}}\right). \qquad (11)$$

Moreover,

$$\psi_s = A_1 B_1 \frac{\pi}{r_{zone}}\sin\left(\frac{\pi x}{H}\right)\cos\left(\frac{\pi y}{r_{zone}}\right), \qquad (12)$$

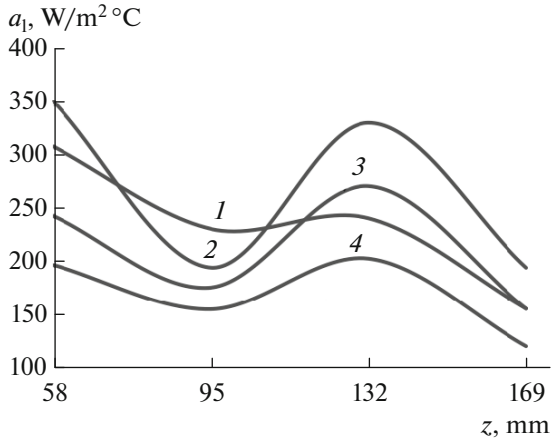

Fig. 7. Variation of the heat transfer coefficient from a bed of aluminosilicate catalyst particles (average diameter 2.5 mm) to a vertical cylindrical heater with a diameter of 42 mm at different air velocities v equal to (*1*) 1.5, (*2*) 2.5, (*3*) 3.5, and (*4*) 4.5 m/s. Reproduced using the data published in [30].

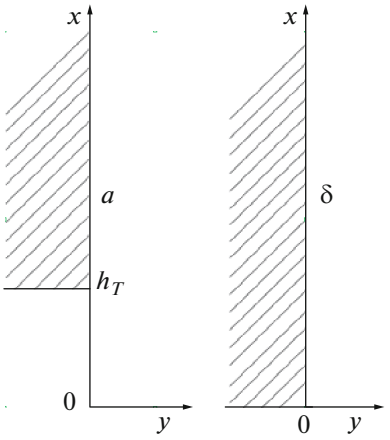

Fig. 8. (a) Real (geometric) and (b) hypothetical location of the immersed body (shaded) in the fluidized bed.

$$\psi_s = -A_l B_l \frac{\pi}{H}\cos\left(\frac{\pi x}{H}\right)\sin\left(\frac{\pi x}{r_{zone}}\right). \quad (13)$$

Let v_s^* be the maximum velocity of a particle in an upward flow (at $y = 0$ and $x = H/2$). Hence,

$$A_l B_l = r_{zone} v_s^* \big/ \pi, \quad (14)$$

$$v_{sx} = v_s^* \sin\left(\frac{\pi x}{H}\right)\cos\left(\frac{\pi y}{r_{zone}}\right), \quad (15)$$

$$v_{sy} = -\frac{r_{zone} v_s^*}{H}\cos\left(\frac{\pi x}{H}\right)\sin\left(\frac{\pi y}{r_{zone}}\right). \quad (16)$$

Let us assume in the first approximation that the maximum velocity of particles in an upward flow is equal to the velocity of gas bubbles floating up in the bed [32, 33], i.e.,

$$v_s^* = U_b, \quad (17)$$

where

$$U_b = v_f - v_{mf}. \quad (18)$$

Using the obtained dependences, the components of the velocity of a particle circulating in the near-surface zone can be easily calculated. It follows from the dependences that the floating of particles is observed near the immersed body, and the sinking of particles is observed at some distance from it. The particle velocity depends on the gas velocity and increases with the growth of the latter. The particle velocity also depends on geometrical characteristics of the bed, such as the height and radius of the near-surface zone, which is determined by the height and diameter of the bed. This dependence is most clearly manifested for radial component v_{sy} of the particle velocity, which apparently indicates the possibility of a decrease in the intensity of particle motion in the radial direction at $r_{zone} \ll H$. As follows from expressions (15) and (16), the v_{sy} value in a real bed used in industrial apparatuses ($r_{zone} < H$) is always less than v_{sx}. With an increase in the gas velocity, bed height H increases and v_{sy} decreases relative to v_{sx}. This should lead to sharp expansion of the bed in the near-surface zone (see Fig. 3) and an increase in the porosity, which leads to a decrease in the intensity of the external heat exchange.

To calculate the average residence time of a particle at a heat exchange surface, one needs to know the most probable path of a particle around a body immersed in a bed. Let us assume that the distribution of the distances traveled by the particles along the heat exchange surface obeys the Gaussian law and take the distribution center at point $S_{av} = H_0$. In this case, the distribution lies within the limits between $S > 0$ and $S < H$. Then the most likely path of a particle along the surface is

$$S = \frac{1}{F - F_0} \times \left\{\frac{\sigma}{\sqrt{2\pi}}\left[e^{-N_1} - e^{-N_2}\right] + \frac{S_{av}}{2}\left[\mathrm{erf}N_1 + \mathrm{erf}N_2\right]\right\}, \quad (19)$$

where

$$N_1 = S_{av}\big/\sqrt{2\sigma}, \quad N_2 = \frac{H - S_{av}}{\sqrt{2\sigma}}, \quad (20)$$

$$F = \frac{1}{2} + \frac{1}{2}\mathrm{erf}\left(\frac{H - S_{av}}{\sigma\sqrt{2}}\right), \quad (21)$$

$$F_0 = \frac{1}{2} + \frac{1}{2}\mathrm{erf}\left(-\frac{S_{av}}{\sigma\sqrt{2}}\right), \quad (22)$$

and σ is the standard deviation.

Table 2. Comparison of the calculated and measured values of the residence time of particles at the surface immersed in a fluidized bed

$v_f = v_{mf}$, m/s	$\bar{\tau}_{calc}$, s	$\bar{\tau}_{meas}$, s
0.0285	2.61	0.399
0.114	0.67	0.287
0171	0.395	0.447
0.228	0.33	0.37
0.285	0.23	0.27

Dependences (19)–(22) were derived by the known methods [34].

Given that the width of the near-surface zone is only seven to eight particle diameters in the bed, one can assume that the particle moves vertically when calculating the residence time of a particle in this zone.

Hence, the average time spent by a particle in the near-surface zone is determined as the quotient from dividing the length of the most probable path of the particle along the vertical surface, which is determined by relations (19)–(22), by the value of the vertical component of the particle velocity determined by expression (15).

Table 2 shows the times of residence of particles at the heat exchange surface for the air–glass system (d_e = 230 μm), which are calculated using the obtained dependences and experimentally measured in [35]. For such particles, the width of the near-surface zone should be 1.8 mm.

As can be seen from Table 2, the calculated and measured values of the residence time of particles at the heat exchange surface approach each other with an increase in the air velocity, i.e., with the formation of the near-surface zone, and the proposed calculation method allows one to estimate this time, which is an important parameter for calculating the intensity of the external heat exchange in a fluidized bed.

CONCLUSIONS

The proposed hypothesis about the existence of a special zone near the heat transfer surface immersed in a fluidized bed and the effect of particle exchange between this zone and the rest of the bed volume on the intensity of the external heat exchange processes in the fluidized bed is experimentally confirmed.

The features of particle motion that were revealed in the indicated near-surface zone have made it possible to develop a method for calculating the residence time of a particle at the heat exchange surface, which is an important parameter for evaluating the intensity of the external heat exchange by means of any of the existing heat transfer models between a pseudofluidized bed and a surface immersed in it.

NOTATION

A, B	constants
C	heat capacity, J/(kg K)
c	constant
D, d	diameter, m
erf	error function
F	aerodynamic force, N
g	gravitational acceleration, m/s^2
H	height of static bed, m
h	distance, m
$\mathbf{i}$	unit vector
K	heat exchange coefficient, W/(m^2 K)
m	weight, kg
p	pressure, Pa
R	motion of particle along radius, m
S	most probable motion, m
T	temperature, K
U, v	velocity, m/s
Z	vertical motion of particle, m
α	heat transfer coefficient, W/(m^2 K)
β	function
$\dot{\gamma}$	shear force, N/m^2
γ	angle of bed repose, rad
ε	bed porosity
λ	effective thermal conductivity, J/(m^2 K)
π	mathematical constant
ρ	density, kg/m^3
σ	standard deviation
τ	time, s
ψ	current function

SUBSCRIPTS AND SUPERSCRIPTS

0	initial value
a	apparatus
av	average value
b	gas bubbles
calc	calculated value
core	core
e	equivalent
meas	measured value
mf	critical value
s	static bed particle
x, y	coordinates of particle position
zone	near-surface zone
$\rightarrow$	random value

FUNDING

This work was supported by the Russian Foundation for Basic Research within project no. 19-58-04004.

REFERENCES

1. Botterill, J.S.M., *Fluid-Bed Heat Transfer,* London: Academic, 1975.
2. Kuipers, J.A.M., Prins, W., and van Swaaij, W.P.M. Numerical calculation of wall-to-bed heat-transfer coefficients in gas fluidized beds, *AIChE J.*, 1992, vol. 38, p. 1079.
3. Martin, H., Heat transfer between gas fluidized beds of solid particles and the surfaces of immersed heat exchanger elements, part I, *Chem. Eng. Process.*, 1984, vol. 18, no. 3, pp. 157–169. https://doi.org/10.1016/0255-2701(84)80005-7
4. Mickley, H.S. and Fairbanks, D.F., Mechanism of heat transfer to fluidized beds, *AIChE J.*, 1955, vol. 1, p. 374.
5. Mickley, H.S., Fairbanks, D.F., and Hawthorn, R.D., The relation between the transfer coefficient and thermal fluctuations in fluidized-bed heat transfer, *Chem. Eng. Prog., Symp. Ser.*, 1961, vol. 57, no. 32, p. 51.
6. Brown, R.C. and Overmann, S.P., The influence of particle thermal time constants on convection coefficients in bubbling fluidized beds, *Powder Technol.*, 1998, vol. 98, p. 13.
7. Yusuf, R., Halvorsen, B., and Melaaen, M.C., Eulerian–Eulerian simulation of heat transfer between a gas–solid fluidized bed and an immersed tube-bank with horizontal tubes, *Chem. Eng. Sci.*, 2011, vol. 66, no. 8, pp. 1550–1564. https://doi.org/10.1016/j.ces.2010.12.015
8. Armstrong, L.M., Gu, S., and Luo, K.H., Study of wall-to-bed heat transfer in a bubbling fluidised bed using the kinetic theory of granular flow, *Int. J. Heat Mass Transfer,* 2010, vol. 53, nos. 21–22, pp. 4949–4959. https://doi.org/10.1016/j.ijheatmasstransfer.2010.05.047
9. Hou, Q.F., Zhou, Z.Y., and Yu, A.B., Gas-solid flow and heat transfer in fluidized beds with tubes: Effects of material properties and tube array settings, *Powder Technol.*, 2016, vol. 296, p. 59.
10. Botterill, J.S.M. and Williams, J.R., The mechanism of heat transfer to gas-fluidized beds, *Trans. Inst. Chem. Eng.*, 1963, vol. 41, p. 217.
11. Koppel, L.B., Patel, R.D., and Holmes, J.T., Statistical models for surface renewal in heat and mass transfer: Part 4. Wall to fluidized bed heat transfer coefficients, *AIChE J.*, 1970, vol. 16, p. 464.
12. Agrawal, S. and Ziegler, E.N., On the optimum transfer coefficient at an exchange surface in a gas-fluidized bed, *Chem. Eng. Sci.*, 1969, vol. 24, no. 8, pp. 1235–1240. https://doi.org/10.1016/0009-2509(69)85044-X
13. Gabor, J.D., Wall-to-bed heat transfer in fluidized beds, *AIChE J.*, 1972, vol. 18, p. 249.
14. Baskakov, A.P., Berg, B.V., Vitt, O.K., Filippovsky, N.F., Kirakosyan, V.A., Goldobin, J.M., and Maskaev, V.K., Heat transfer to objects immersed in fluidized beds, *Powder Technol.*, 1973, vol. 8, p. 273.
15. Ozkaynak, T.F. and Chen, J.C., Emulsion phase residence time and its use in heat transfer models in fluidized beds, *AIChE J.*, 1980, vol. 26, p. 544.
16. Rhodes, M., Mineo, H., and Hirama, T., Particle motion at the wall of a circulating fluidized bed, *Powder Technol.*, 1992, vol. 70, p. 207.
17. Molerus, O., Burschka, A., and Dietz, S., Particle migration at solid surfaces and heat transfer in bubbling fluidized beds – 1. Particle migration measurement systems, *Chem. Eng. Sci.*, 1995, vol. 50, p. 871.
18. Noymer, P.D. and Glicksman, L.R., Cluster motion and particle-convective heat transfer at the wall of a circulating fluidized bed, *Int. J. Heat Mass Transfer,* 1998, vol. 41, p. 147.
19. Ziegler, E.N., Koppel, L.B., and Brazelton, W.T., Effect of solid thermal properties on heat transfer to gas fluidized beds, *Ind. Eng. Chem. Fundam.*, 1964, vol. 3, p. 324.
20. Borodulya, V.A., Teplitskii, Yu.S., Ganzha, V.L., and Makarevich, I.I., Modeling of external and interphase heat transfer processes in dispersion media, *Teplomassoobmen – Minskii mezhdunarodnyi forum (24–27 maya 1988 g.). Sektsii 4, 5. Teplomassoobmen v dvukhfaznykh i dispersnykh sistemakh: problemnye doklady* (Heat and Mass Transfer: The Minsk International Forum (May 24–27, 1988). Sections 4 and 5. Heat and Mass Transfer in Two-Phase and Disperse Systems: Key Lectures) (Minsk, 1988), Minsk: Inst. Teplo- i Massoobmena im. A.V. Lykova Akad. Nauk B. SSR, 1988, p. 122.
21. Antonishin, N.V. and Lushchikov, V.V., Heat transfer in dispersion media, in *Protsessy perenosa v apparatakh s dispersnymi sistemami. Sbornik nauchnykh trudov ITMO im. A.V. Lykova AN BSSR* (Transport Processes in Apparatuses with Disperse Systems: A Collection of Scientific Papers of the Luikov Heat and Mass Transfer Institute, Academy of Sciences of the Belorussian SSR), Minsk: Inst. Teplo- i Massoobmena im. A.V. Lykova Akad. Nauk B. SSR, 1986, p. 3.
22. Borodulya, V.A., Teplitskii, Yu.S., Markevich, I.I., Khassan, A.F., and Eremenko, T.P., Heat transfer between a fluidized bed and the surface, *J. Eng. Phys.*, 1990, vol. 58, no. 4, pp. 446–452. https://doi.org/10.1007/BF00877352
23. Antonishin, N.V. and Lushchikov, V.V., Degeneration of the effect of the disperse structure of a bed on heat exchange with the surface, *Teplomassoobmen – Minskii mezhdunarodnyi forum (24–27 maya 1988 g.). Sektsii 4, 5. Teplomassoobmen v dvukhfaznykh i dispersnykh sistemakh: problemnye doklady* (Heat and Mass Transfer: The Minsk International Forum (May 24–27, 1988). Sections 4 and 5. Heat and Mass Transfer in Two-Phase and Disperse Systems: Key Lectures) (Minsk, 1988), Minsk: Inst. Teplo- i Massoobmena im. A.V. Lykova Akad. Nauk B. SSR, 1988, p. 159.
24. Xavier, A.M. and Davidson, J.F., Heat transfer in fluidized beds: Convective heat transfer in fluidized beds, *Fluidization,* Davidson, J.F., Clift, R., and Harrison, D., Eds., London: Academic, 1985, p. 437.
25. Gabor, J.D., Wall-to-bed heat transfer in fluidized and packed beds, *Chem. Eng. Prog., Symp. Ser.*, 1970, vol. 66, no. 105, p. 76.

26. Buevich, Yu.A., in *Teplomassoobmen-VI. Tezisy dokladov Nauchnoi konferentsii. Problemnye doklady VI Vsesoyuznoi konferentsii po teplomassoobmenu. Chast' 2* (Heat and Mass Transfer-VI: Abstracts of Papers Presented at the VI All-Russian Conference on Heat and Mass Transfer: Key Lectures: Part 2) (Minsk, 1981), Minsk: Inst. Teplo- i Massoobmena im. A.V. Lykova Akad. Nauk B. SSR, 1981, p. 54.

27. Korolev, V.N., Structural and gas-dynamic conditions and external heat transfer in fluidized media, *Extended Abstract of Doctoral (Eng.) Dissertation,* Sverdlovsk: Inst. of Thermal Physics, Academy of Sciences of the USSR, 1988.

28. Kondukov, N.B., Frenkel', L.I., Nagornov, S.A., Romanenko, N.Ya., and Tarov, V.P., Some features of hydrodynamics and external heat transfer in a fluidized bed, *Dokl. Akad. Nauk SSSR,* 1975, vol. 224, no. 5, p. 1138.

29. Frenkel', L.I. and Kondukov, N.B., Study of gas velocity profiles in a monodisperse fluidized bed, *Khim. Prom-st.*, 1966, no. 6, p. 418.

30. Nagornov, S.A., Intensification of heat transfer in inhomogeneous fluidized and vibrocirculating media, *Doctoral (Eng.) Dissertation,* Tambov: All-Russian Scientific Research Inst. for the Use of Machinery and Oil Products in Agriculture, 2003.

31. Protod'yakonov, I.O. and Chesnokov, Yu.G., *Gidromekhanika psevdoozhizhennogo sloya* (Hydromechanics of Fluidized Beds), Leningrad: Khimiya, 1982.

32. Grace, J.R. and Harrison, D., The influence of bubble shape on the rising velocities of large bubbles, *Chem. Eng. Sci.*, 1967, vol. 22, no. 10, p. 1337.

33. Rowe, P.N. and Everett, D.J., Fluidised bed bubbles viewed by X-rays: Part II—The transition from two to three dimensions of undisturbed bubbles, *Trans. Inst. Chem. Eng.*, 1972, vol. 50, no. 1, pp. 49–54.

34. Korn, G. and Korn, T., *Spravochnik po matematike* (Handbook of Mathematics), Moscow: Nauka, 1977.

35. Selzer, V.W. and Tomson, W.J., Fluidized bed heat transfer: The packet theory revisited, *AIChE Symp. Ser.*, 1977, vol. 73, no. 161, pp. 29–37.

Translated by O. Kadkin